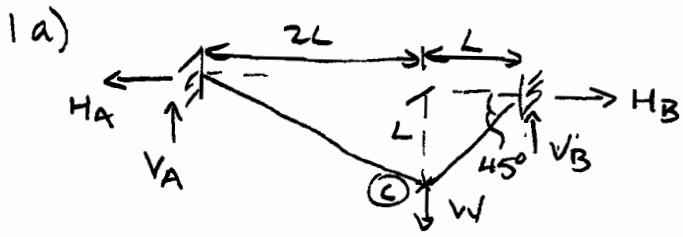


PART 1A ENGINEERING TRIPOS  
PAPER 2 - STRUCTURES & MATERIALS  
SECTION A - CRIB 2007/2008  
JANET LEES

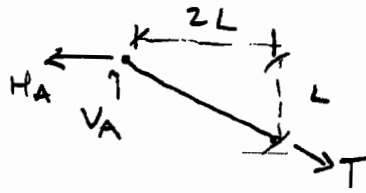
Q1 1/1



$$\sum M_A = 0 \rightarrow V_B \cdot 3L - W \cdot 2L = 0 \quad \therefore V_B = \frac{2}{3}W \uparrow$$

$$\sum V = 0 \rightarrow V_A + V_B = 0 \quad \therefore V_A = \frac{1}{3}W \uparrow$$

FBD OF AC



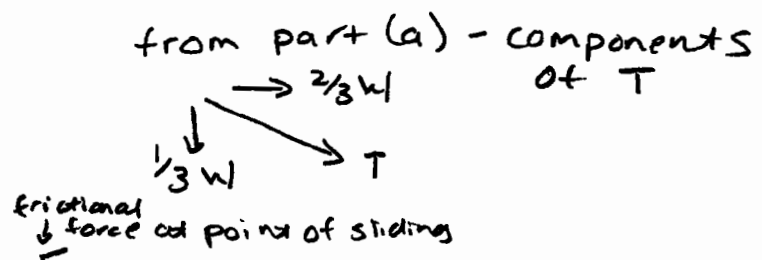
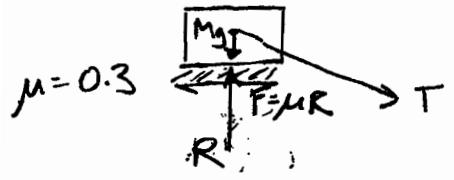
$$\sum M_C = 0 \rightarrow H_A \cdot L - V_A \cdot 2L = 0 \quad \therefore H_A = \frac{2}{3}W \leftarrow$$

$$H_A = 2V_A$$

$$\sum H = 0 \rightarrow -H_A + H_B = 0 \quad \therefore H_B = \frac{2}{3}W \rightarrow$$

$$H_A = H_B$$

b) FBD at A

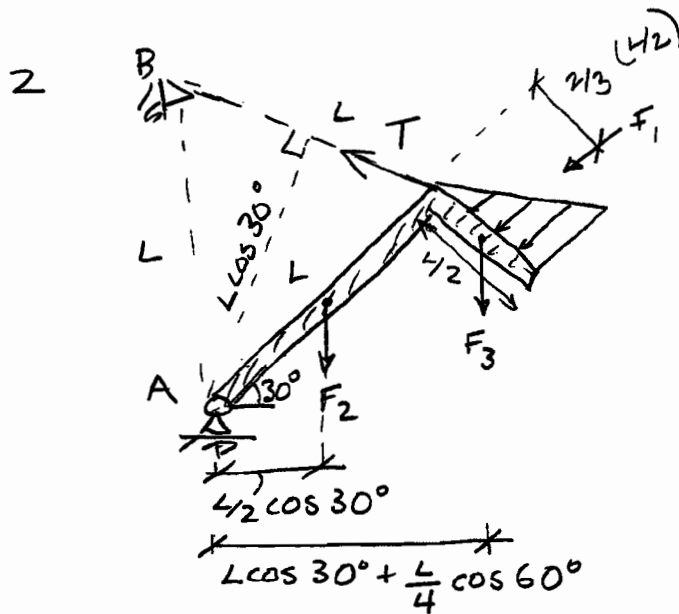


$$R = Mg + \frac{W}{3}, \quad F = \mu R = H$$

for sliding not to occur when the applied horizontal component  $H = \frac{2}{3}W$

$$\mu (Mg + \frac{W}{3}) = \frac{2}{3}W \quad \therefore M = 0.193W$$

$$M = \frac{17W}{9g}$$



$$F_1 = 10 \text{ kN/m} \times 5 \text{ m} / 2 \times 1/2 = 12.5 \text{ kN}$$

$$F_2 = 30 \text{ kN}, \quad F_3 = W/2 = 15 \text{ kN}$$

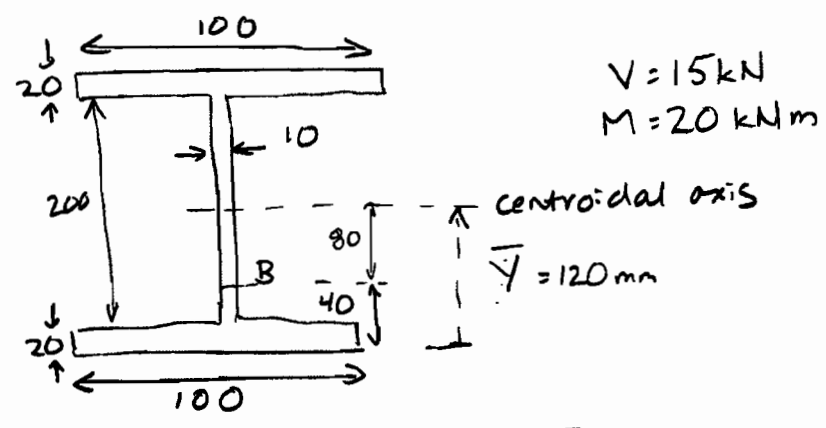
$$\begin{aligned} \sum M_A = 0 \Rightarrow & F_2 \times \frac{L}{2} \cos 30^\circ + F_3 \left( L \cos 30^\circ + \frac{L}{4} \cos 60^\circ \right) \\ & + F_1 \left( \frac{2}{3} \cdot \frac{L}{2} \right) - T \cdot L \cos 30^\circ = 0 \end{aligned}$$

$$\begin{aligned} \therefore & 30 \times \frac{5}{2} \times \frac{\sqrt{3}}{2} + 15 \times \left( \frac{5\sqrt{3}}{2} + \frac{5}{8} \right) + 12.5 \times \frac{5}{3} \\ & - T \times 5 \times \frac{\sqrt{3}}{2} = 0 \end{aligned}$$

$$\therefore T = 36.98 \text{ kN}$$

Many students recognised that the most direct way to solve the problem was to make a cut through the cable and take moments about A. Students who tried to resolve forces in the horizontal and vertical directions had a tendency to overlook the support reactions in their free body diagrams which lead to errors. The triangular load caused some difficulties in terms of finding the resultant force and location.

3



symmetric section therefore  $\bar{Y} = 120 \text{ mm}$

$$I = \frac{b_o d_o^3}{12} - \frac{b_i d_i^3}{12} = \frac{100 \times 240^3}{12} - \frac{90 \times 200^3}{12}$$

$$= 55.2 \times 10^6 \text{ mm}^4$$

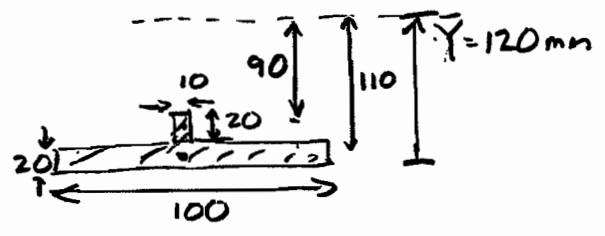
(a)  $\sigma = \frac{M y}{I}$  ← distance from centroidal axis

$$= \frac{20 \times 10^6 \times (120 - 40)}{55.2 \times 10^6} = 29 \text{ MPa}$$

(b)  $\tau = \frac{S A_c \bar{y}}{I a}$  ← first moment of area of the cut off portion about the centroidal axis

$$A_c \bar{y} = 20 \times 10 \times 90 + 20 \times 100 \times 110$$

$$\therefore A_c \bar{y} = 238000 \text{ mm}^3$$



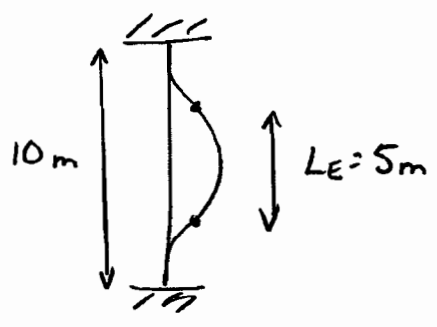
$$\tau = \frac{15000 \times 238000}{55.2 \times 10^6 \times 10}$$

← length of cut in plane of the cross-section

$$= 6.47 \text{ MPa}$$

The majority of mistakes could be attributed to applying formulae without thinking about the constituent terms. This was particularly noticeable when determining the  $A_c \bar{y}$  term required to calculate the shear stress.

4 a)



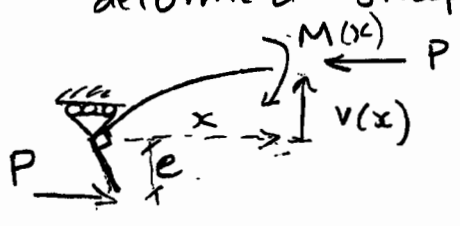
UC 356 x 368 x 177  
 $I_{yy} = 20530 \text{ cm}^4$   
 use  $I$  in weakest direction  
 from Structures Database

for steel,  $E = 210000 \text{ MPa}$

$$P_{ER} = \frac{\pi^2 EI}{L_e^2} = \frac{\pi^2 \times 210000 \times 20530 \times 10^4}{(5000)^2}$$

$$= 17.02 \times 10^6 \text{ N} = 17.02 \text{ MN}$$

b) For buckling, consider FBD in deformed shape



sign convention used  
 ↻ +ve M, K  
 ↑ v +ve

$$M(x) = P(v(x) + e)$$

(Note - any consistent sign convention is acceptable)

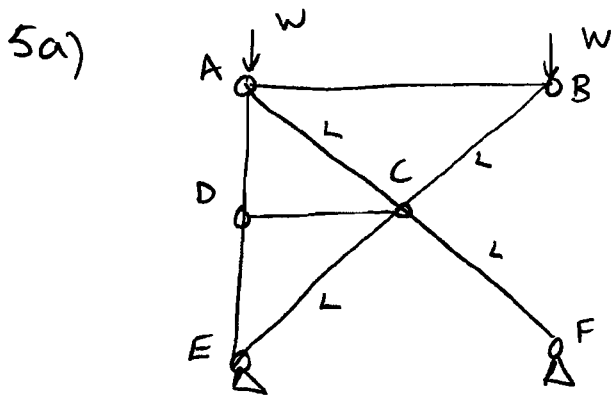
$$M = EI \Delta K$$

$$\text{where } \Delta K = -\frac{d^2 v}{dx^2}$$

$$\therefore Pv + Pe = -EI \frac{d^2 v}{dx^2}$$

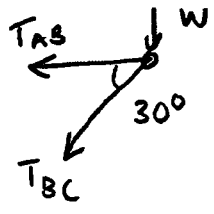
$$\frac{EI}{P} \cdot \frac{d^2 v}{dx^2} + v = -e$$

Common errors were in determining the effective length and the weakest axis of bending. Part (b) was either done very well or very poorly. Students who carefully set up a free body in the deformed shape generally solved the question correctly.



· find member forces

FBD - Joint B (easiest to start with joint with only 2 unknowns)



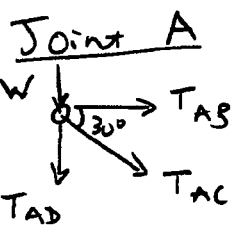
$$\sum V = 0 \quad -T_{BC} \sin 30^\circ - W = 0$$

$$T_{BC} = -2W$$

$$\sum H = 0 \quad -T_{AB} - T_{BC} \cos 30^\circ = 0$$

$$T_{AB} = -T_{BC} \cos 30^\circ$$

$$= \sqrt{3}W$$



$$\sum H = 0 \quad T_{AB} + T_{AC} \cos 30^\circ = 0$$

$$T_{AC} = -T_{AB} / \cos 30^\circ$$

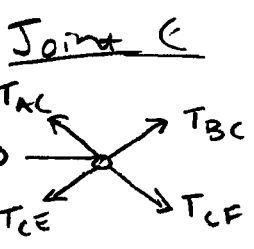
$$= -2W$$

$$\sum V = 0 \quad -T_{AC} \sin 30^\circ - W - T_{AD} = 0$$

$$T_{AD} = 0$$

As  $T_{AD} = 0$ ,  $T_{DE} = 0$

By inspection  $T_{DC} = 0$  ( $\sum H = 0$ )



$$\sum H = 0 \quad -T_{AC} \cos 30^\circ + T_{BC} \cos 30^\circ - T_{CE} \cos 30^\circ + T_{CF} \cos 30^\circ = 0$$

$$\therefore T_{CE} = T_{CF}$$

$$\sum V = 0 \quad T_{AC} \sin 30^\circ + T_{BC} \sin 30^\circ - T_{CE} \sin 30^\circ - T_{CF} \sin 30^\circ = 0$$

$$T_{CE} = T_{CF} = -2W$$

(also by symmetry)

5a) continued

	T	L	$e = TL/EA$	$T^*$	$T^*e$
$T_{AB}$	$\sqrt{3}W$	$\sqrt{3}L$	$3WL/EA$	$\sqrt{3}$	$3\sqrt{3}WL/EA$
$T_{BC}$	$-2W$	$L$	$-2WL/EA$	$-2$	$4WL/EA$
$T_{CF}$	$-2W$	$L$	$-2WL/EA$	$-2$	$4WL/EA$
$T_{CE}$	$-2W$	$L$	$-2WL/EA$	$-2$	$4WL/EA$
$T_{AD}$	$0$	$L/2$	$0$	$1$	$0$
$T_{DC}$	$0$	$\sqrt{3}L/2$	$0$	$0$	$0$
$T_{DE}$	$0$	$L/2$	$0$	$1$	$0$
$T_{AC}$	$-2W$	$L$	$-2WL/EA$	$-2$	$4WL/EA$

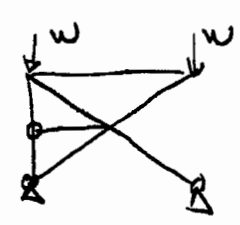
After finding member forces, can then calculate bar extensions using  $e = TL/EA$

Can then use a displacement diagram or Virtual work to solve for  $\delta_B$ . The Virtual Work solution is detailed below

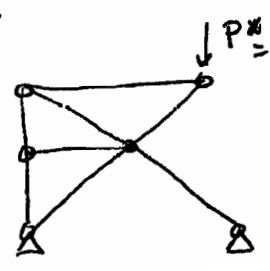
V.W. 
$$\underbrace{\sum P \cdot \delta}_{\text{equilibrium set}} = \underbrace{\sum T \cdot e}_{\text{compatible set}}$$

looking to find displacements so compatible set is real, equilibrium set is virtual

As vertical displacements at B are required, use a virtual downwards force at B as virtual system.

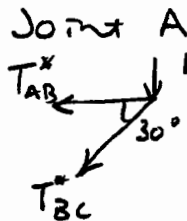
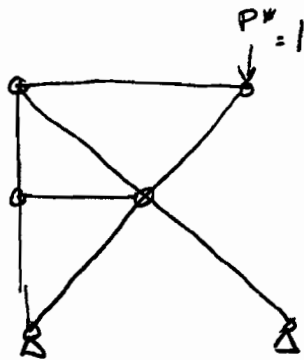


to find real extensions



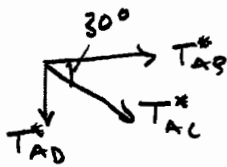
to find Virtual forces

5a) continued - find virtual forces and include in table on previous page



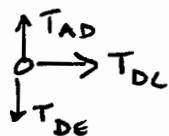
$$\left. \begin{aligned} \sum V = 0 \\ \sum H = 0 \end{aligned} \right\} \rightarrow \begin{aligned} T_{BC}^* &= -2 \\ T_{AB}^* &= \sqrt{3} \end{aligned}$$

Joint B

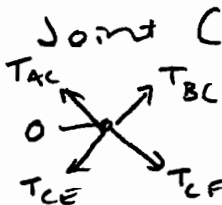


$$\left. \begin{aligned} \sum V = 0 \\ \sum H = 0 \end{aligned} \right\} \rightarrow \begin{aligned} T_{AC}^* &= -2 \\ T_{AD}^* &= 1 \end{aligned}$$

Joint D



$$\left. \begin{aligned} \sum V = 0 \\ \sum H = 0 \end{aligned} \right\} \rightarrow \begin{aligned} T_{DE}^* &= 1 \\ T_{DC}^* &= 0 \end{aligned}$$



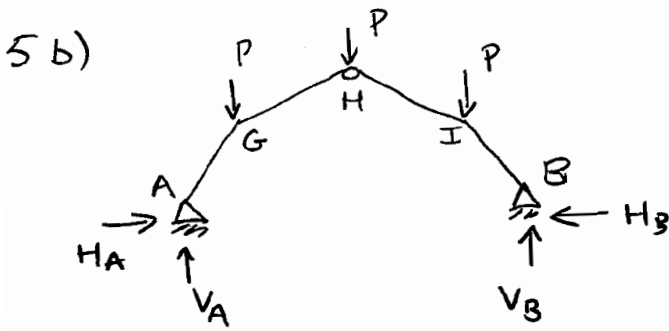
$$\left. \begin{aligned} \sum V = 0 \\ \sum H = 0 \end{aligned} \right\} \rightarrow \begin{aligned} T_{CE}^* &= -2 \\ T_{CF}^* &= -2 \end{aligned}$$

V.W.

$$\sum P^* \cdot \delta = \sum T^* \cdot e$$

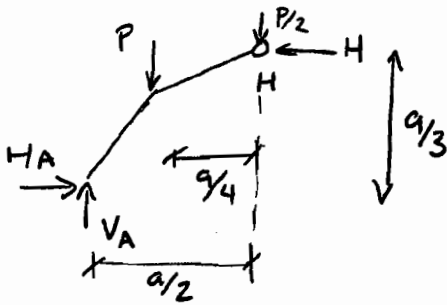
$$1 \cdot \delta_B = \frac{WL}{EA} (3\sqrt{3} + 4 + 4 + 4 + 4)$$

$$\begin{aligned} \delta_B &= (16 + 3\sqrt{3}) \frac{WL}{EA} \text{ downwards} \\ &= 21.2 \frac{WL}{EA} \downarrow \end{aligned}$$



from symmetry  $V_A = V_B = 3P/2 \uparrow$

FBD of A-G-H

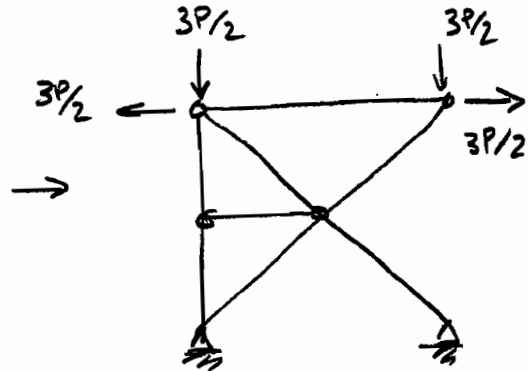
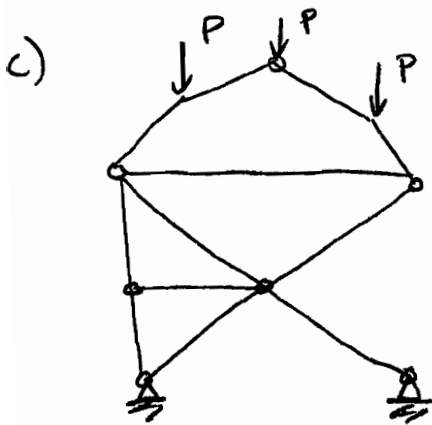


$\sum M_H = 0$

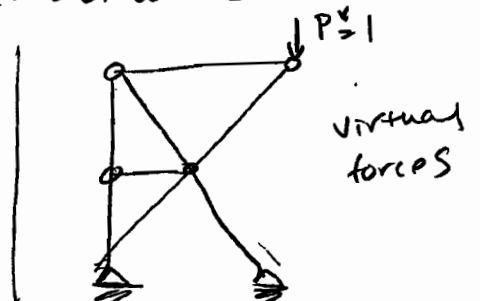
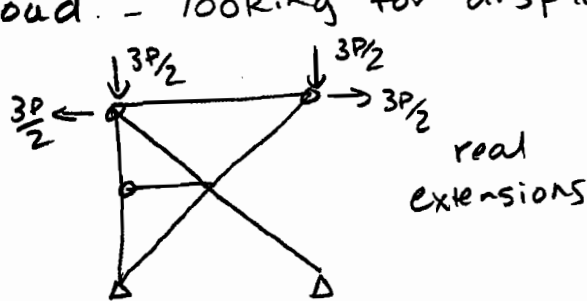
$H_A \cdot \frac{a}{3} - V_A \cdot \frac{a}{2} + P \cdot \frac{a}{4} = 0$

$H_A \cdot \frac{a}{3} = \frac{P a}{2} \therefore H_A = \frac{3P}{2} \rightarrow$

$\sum H = 0 \therefore H_B = \frac{3P}{2} \leftarrow$

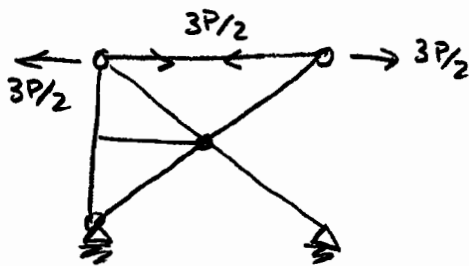


Same as part (a) but with additional horizontal load and scaled vertical load. - looking for displacement at B





5c) continued



consider horizontal component in isolation  $\rightarrow$  horizontal load only causes force in  $T_{AB}$

$\therefore$  New table including horizontal thrust and using  $W = 3P/2$

	T	L	e (all $\times \frac{PL}{EA}$ )	T*	T* e (as before $\frac{xPL}{EA}$ )
$T_{AB}$	$(3\sqrt{3}/2 + 3/2)P$	$\sqrt{3}L$	$(9+3\sqrt{3})/2$	$\sqrt{3}$	$(9\sqrt{3}+9)/2$
$T_{BC}$	$-3P$	L	-3	-2	6
$T_{CF}$	$-3P$	L	-3	-2	6
$T_{CE}$	$-3P$	L	-3	-2	6
$T_{AD}$	0	$L/2$	0	1	0
$T_{DC}$	0	$\sqrt{3}L/2$	0	0	0
$T_{DE}$	0	$L/2$	0	1	0
$T_{AC}$	$-3P$	L	-3	-2	6

$$\sum P \cdot \delta = \sum T \cdot e$$

$$1 \cdot \delta = \frac{PL}{EA} \left( \frac{9\sqrt{3}+9}{2} + 4 \times 6 \right)$$

$$\delta_B = \left( \frac{57+9\sqrt{3}}{2} \right) \frac{PL}{EA} \text{ downwards } \downarrow$$

$$= 36.3 \frac{PL}{EA} \downarrow$$

## 5c) Alternative solution

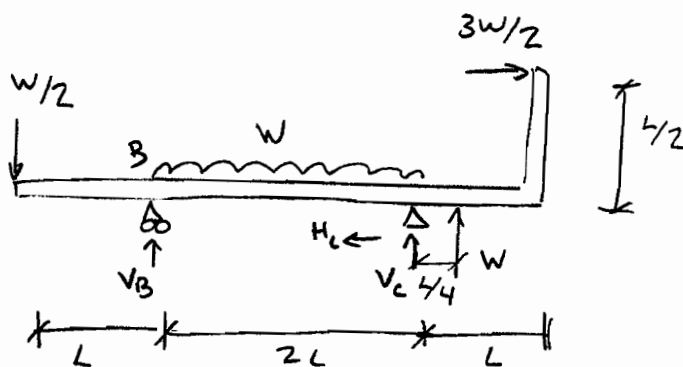
Good students spotted that the solution is simply the answer from (a) plus an additional term where

$$\begin{aligned}
 \delta_B &= \underbrace{\sum T^* e \left( \frac{3P/2}{W} \right)}_{\text{from (a)}} + \underbrace{\frac{3P}{2} \cdot \frac{\sqrt{3}L}{EA}}_{\text{extension}} \cdot \sqrt{3} \quad T^* \\
 &= (3\sqrt{3} + 16) \frac{WL}{EA} \cdot \frac{3P}{2W} + \frac{3PL}{2EA} \cdot 3 \\
 &= \frac{9\sqrt{3} + 57}{2} \frac{PL}{EA}
 \end{aligned}$$

An unfortunately large minority of students wrote down a series of forces with no indication of where they came from and did not identify their real and virtual systems. This often led to mistakes and confusion. In contrast, those who did consider and present their work in a coherent fashion generally did very well.

Q6 1/4

6.



(a)

$$\sum M_B = 0 \quad \text{+ve } \curvearrowright \quad -\frac{W \cdot L}{2} + W \cdot L - V_C \cdot 2L - W \frac{9L}{4} + \frac{3WL}{4} = 0$$

$$V_C \cdot 2L = -\frac{2WL}{4} + \frac{4WL}{4} - \frac{9WL}{4} + \frac{3WL}{4}$$

$$V_C \cdot 2L = -\frac{4WL}{4} \quad \therefore V_C = -\frac{W}{2}$$

$$\sum M_C = 0 \quad \text{+ve } \curvearrowright \quad V_B \cdot 2L - \frac{W}{2} \cdot 3L - W \cdot L + \frac{WL}{4} + \frac{3WL}{4} = 0$$

$$V_B \cdot 2L = \frac{6WL}{4} + \frac{4WL}{4} + \frac{WL}{4} - \frac{3WL}{4}$$

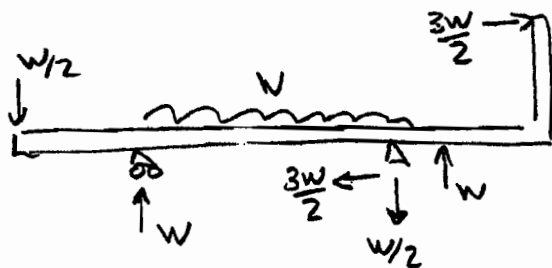
$$V_B \cdot 2L = \frac{8WL}{4} \quad \therefore V_B = W$$

check

$$\sum V = 0 \quad \text{+ve } \uparrow \quad -\frac{W}{2} + V_B - W + V_C + W = 0$$

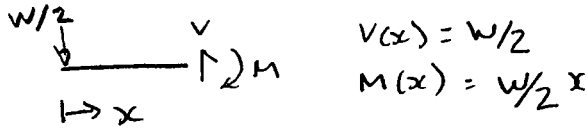
$$V_B = -V_C + W/2 \quad \checkmark$$

$$\sum H = 0 \quad H_C = 3W/2 \quad (\text{in direction indicated})$$

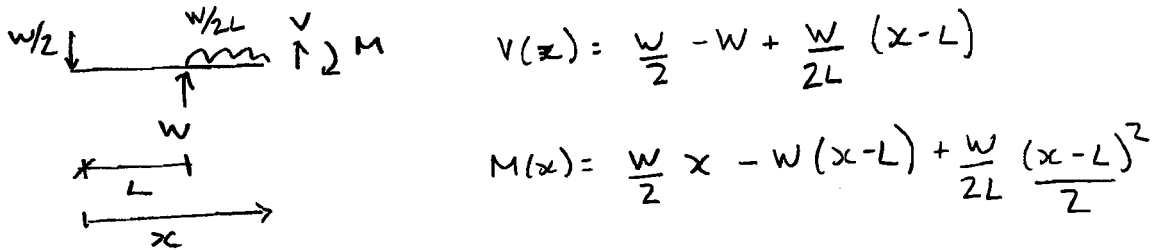


6 (b)

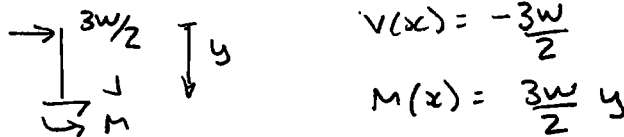
FBD A-B  $x < L$



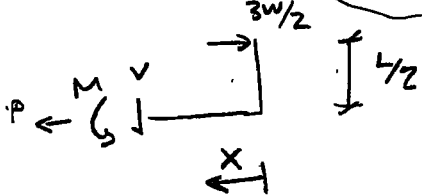
FBD A-C  $L < x < 3L$



FBD E-D - vertical piece



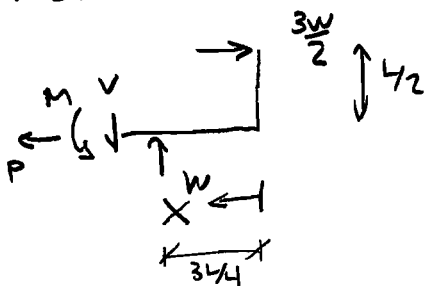
FBD ED  $x < \frac{3L}{4}$



easier to use origin from RH end  
axial force  
 $P = \frac{3W}{2}$

$V(x) = 0$   
 $M(x) = \frac{3WL}{4}$

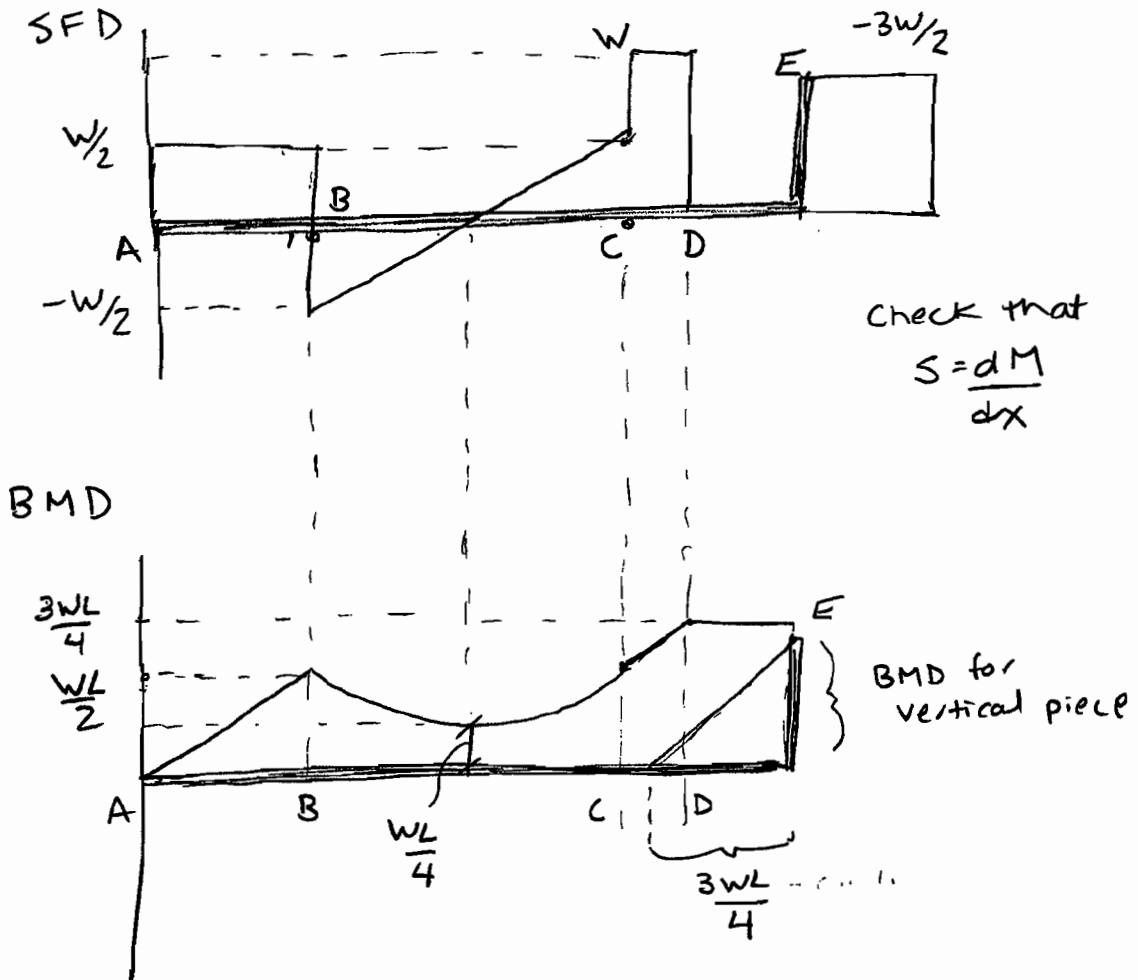
FBD E-C  $L > x > \frac{3L}{4}$



$V(x) = W$   
 $M(x) = \frac{3WL}{4} - W(x - \frac{3L}{4})$

$P = \frac{3W}{2}$

6 b) continued



Check  $M_{MIDSPAN}$

From FBD A-C  $L < x < 3L$

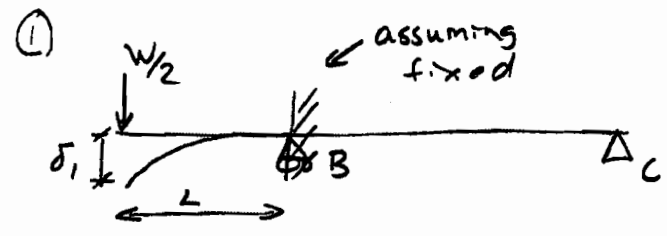
$$V(2L) = \frac{W}{2} - W + \frac{W}{2L} (2L - L) = 0$$

$$M(2L) = \frac{W \cdot 2L}{2} - W(2L - L) + \frac{W}{2L} \frac{(2L - L)^2}{2}$$

$$= WL - WL + \frac{W}{4L} (L^2) = \frac{WL}{4}$$

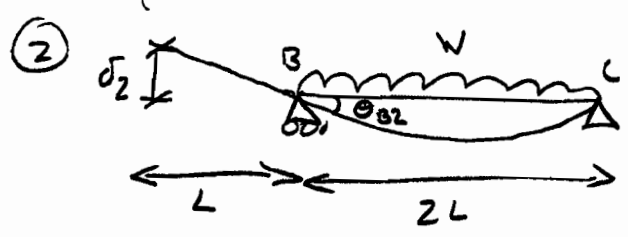
There was evidence of bending moment and shear force diagrams being constructed with little or no obvious calculation which led to errors. In part (c) most students calculated the 'cantilever' component of the deflection at A. However, a much smaller number recognised the need to incorporate an additional rotation at B and the majority overlooked at least one or more of the components that would contribute to this rotation.

6 c) - superposition of structures databook cases  
Vertical displacement is sum of four terms

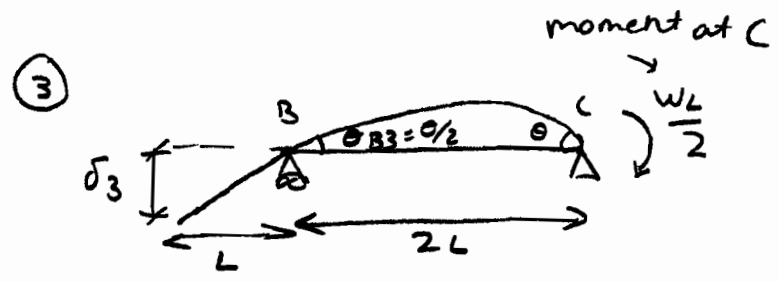


$$\delta_1 = \frac{(W/2)L^3}{3EI} = \frac{WL^3}{6EI}$$

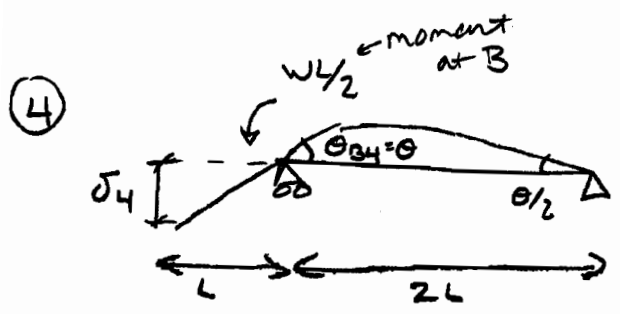
+ rotation at B terms



$$\begin{aligned} \delta_2 &= -\theta_{B2} \cdot L \\ &= -\frac{W(2L)^2}{24EI} \cdot L \\ &= -\frac{WL^3}{6EI} \end{aligned}$$



$$\begin{aligned} \delta_3 &= \theta_{B3} \cdot L \\ &= \frac{(WL/2) \cdot 2L}{3EI} \cdot \left(\frac{1}{2}\right) \cdot L \\ &= +\frac{WL^3}{6EI} \end{aligned}$$



$$\begin{aligned} \delta_4 &= \theta_{B4} \cdot L \\ &= \frac{WL \cdot 2L}{2} \cdot \frac{1}{3EI} \\ &= +\frac{WL^3}{3EI} \end{aligned}$$

assuming +ve ↓

$$\begin{aligned} \delta_A &= \delta_1 + \delta_2 + \delta_3 + \delta_4 \\ &= \frac{WL^3}{EI} \left( \frac{1}{6} - \frac{1}{6} + \frac{1}{6} + \frac{1}{3} \right) = \frac{WL^3}{2EI} \downarrow \text{downwards} \end{aligned}$$

## PART 1A ENGINEERING TRIPOS 2008

### PAPER 2 STRUCTURES AND MATERIALS Examiner: P W R Beaumont

#### SECTION B CRIB

*(This crib provides thorough answers to the descriptive questions that go further than can be expected of the candidate in the time allotted. Answers to the descriptive parts of questions should contain some of the important points below).*

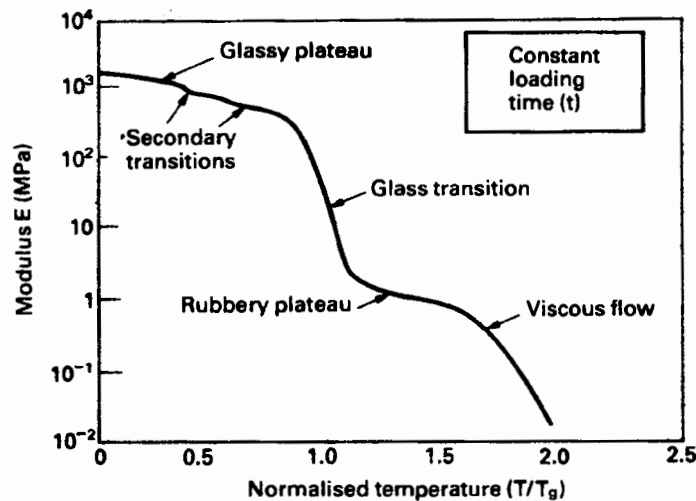
7. (a-c) The properties of materials depend on their structure across a spectrum of size-scale: atomistic structure, microscopic structure, and macroscopic size scales, (component shape and volume). Generally, metals are of fcc, bcc, or cph atomic structure with a variety of slip planes and slip directions. Unlike metals, bonding in ceramics is ionic or covalent, and unlike metals there are no free electrons, and their bonds are extremely strong.

The tensile fracture of brittle materials such as ceramics occurs by fast fracture from small (usually intrinsic) defects. In compression, the defects close up, and fast fracture cannot occur. Instead, crack faces shear relative to one another, generating wing cracks at the crack ends. The wing cracks tend to be aligned parallel to the loading direction. Failure occurs by the progressive spreading and interlinking of cracks, leading to a general crushing failure at a much higher stress. Only at high temperature is a limited amount of plasticity in ceramics possible by grain boundary sliding, for example. Cracks eventually nucleate at the grain boundary. In tension, the largest flaw in the ceramic propagates fast. Inherent cracks perpendicular to the applied stress direction propagate unstably in tension. In compression, many flaws extend slowly, leading to crushing. In compression the off-axis crack in shear extends stably (slowly) away from its original orientation to becoming parallel to the compressive stress axis. Eventually, the ceramic begins to crush and fragment by the coalescence of these slowly growing micro-cracks. In other words, fracture in compression does not start from a single crack but from the slow extension of many cracks, and their accumulation. It is the average flaw size  $a_{av}$  that affects the ultimate *compressive* strength.

Thermoplastics are *amorphous* like polymethylmethacrylate, PMMA, and polycarbonate, PC), or *crystalline* like polyethylene, PE, and Nylon (which are really only partly crystalline). Thermosetting are highly-*crosslinked* amorphous systems like epoxy resin, polyester resin, and other adhesives. All are long, entangled chain molecules, so-called macromolecules, resembling a long, entangled thread, rope, or wire. The 3-D macromolecular solid is made up of these long chains, having a *covalent* -C-C- back-bone held together by a network of covalent cross-links, weaker VDW forces and H<sub>2</sub> bonds. Thermoplastics have: a range of molecular weights, lengths of chains, packing geometries, variations of molecular architecture, side arms, bulky groups. They have no sharp melting point. Every thing is *temperature sensitive*.

Basically, there are 5 methods of stiffening the polymer: cross-linking, crystallisation, chain alignment, chain stiffening, chain branching. The stiffness of a polymer depends on: molecular weight distribution, crystallinity, (affected by side branches), spherulite size and volume fraction, flow or alignment effects (anisotropic structure), chemical structure (X-link density, side branches, etc), temperature (and/or strain-rate).

(d) The Modulus-Temperature diagram below shows a massive drop in stiffness (1000 times) over a small temperature range, the glass transition temperature  $T_g$ . A drop in modulus by a factor of 2 may occur below the  $T_g$ . A highly crosslinked or a highly crystalline polymer does not undergo such a dramatic change of property at the  $T_g$ . In fact, a highly xlinked resin does not have a  $T_g$ , it simply starts to burn at elevated temperature! At the  $T_g$ , there is change in "free volume" of the polymer ("space between the atoms") which permits segments or particular groupings of the polymer chains to move with respect to each other. Linear-amorphous polymers have 4 regimes of deformation followed by definite melting (or decomposition): glassy,  $E$  about 3 GPa; glass transition,  $E$  drops 1000 times; rubbery,  $E$  about 3 MPa; viscous. Modulus of the plateau at temperatures greater than  $T_g$  increases with increasing crystallinity, or cross-link density.

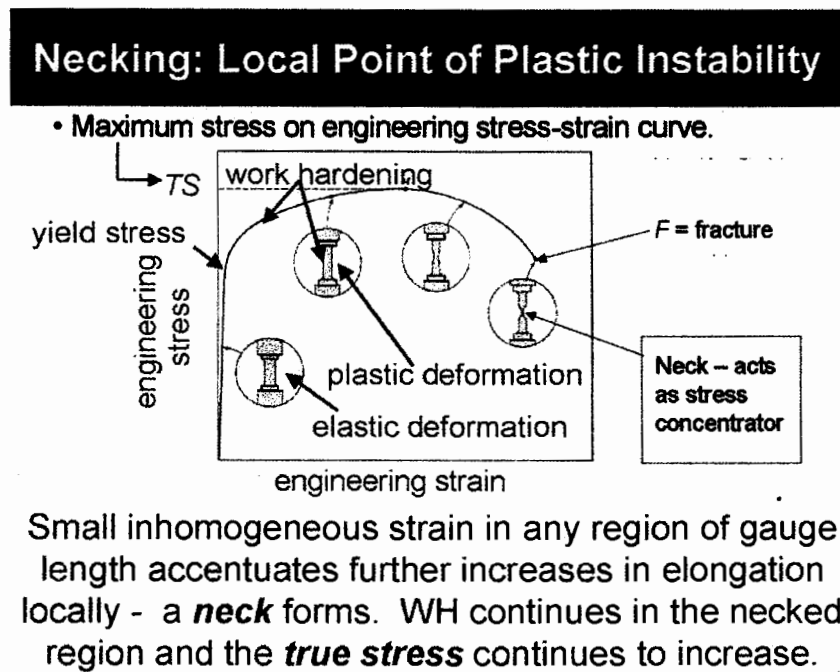
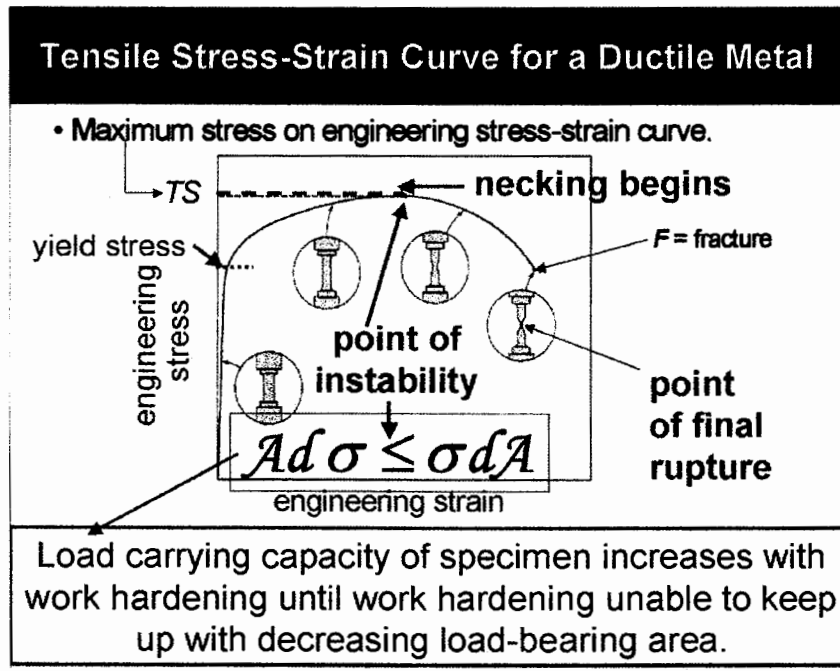


Stiffness (modulus) vs Temperature and Transitions in amorphous polymers

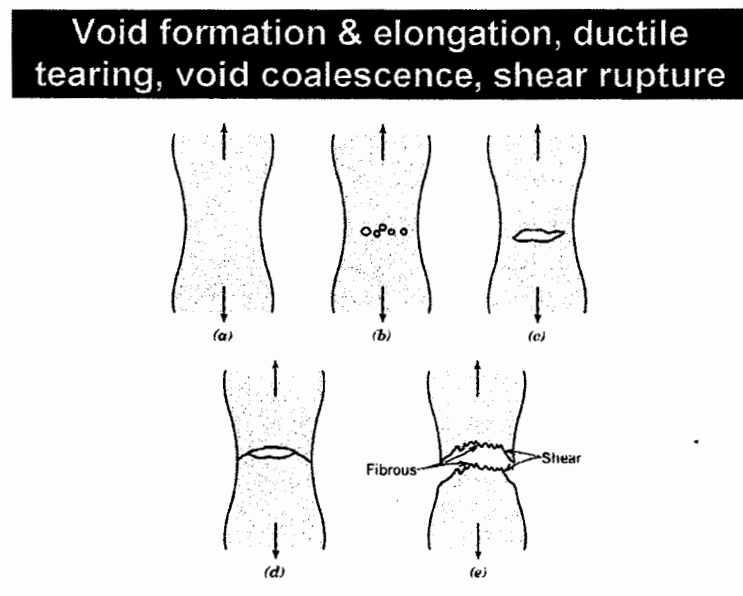
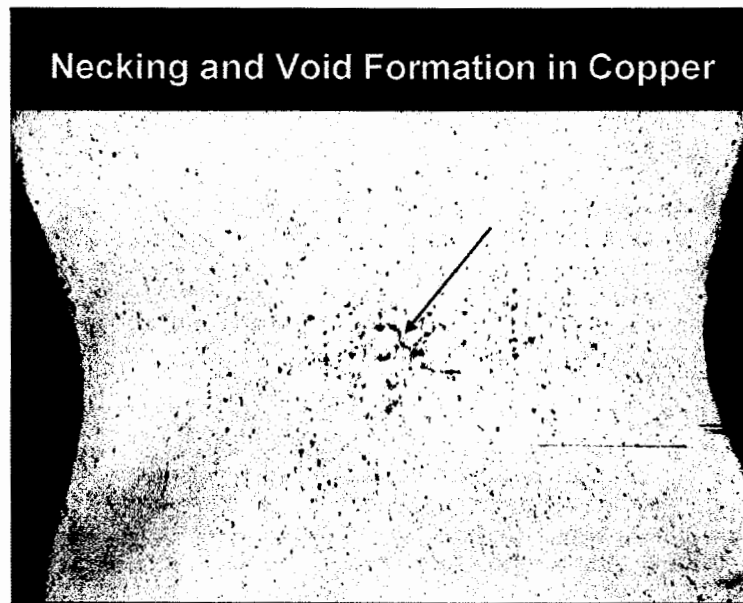
At very high values of crystallinity or cross-link density, the polymer does not have a glass transition and the modulus remains high until melting or degradation. Many thermoplastics are semicrystalline. The spherulites that form the crystalline phase are capable of unravelling even below the  $T_g$  so not all flow processes are "frozen" out. Secondary transitions (particular mechanisms or processes of molecular motion) can occur at  $T$  less than  $T_g$  (the primary transition temperature) and impart some ductility and toughness. The rotation of side groups imparts some ductility and toughness to the polymer below the polymer's principle glass transition temperature,  $T_g$ . At  $T_g$ , the "glass transition", increasing temperature melts weaker bonds and chain segments slip easily;  $E$  drops steeply and reptation or viscous sliding (think of a polymer chain within a flexible tube) is easy above  $T_g$ .



8. A summary of the answers to the questions raised (a-e) is shown in the stress-strain curves below. Full marks could be obtained by making similar sketches and labelling the curves as indicated.



These sketches below might be included although not essential to score full marks.



9. (a) and (b) The galvanic series ranks the corrosion potentials of common metals in sea water. The metal with the more negative potential will become the anode when connected to another metal which becomes the cathode. Furthermore, the greater this difference between potentials of the 2 metals in contact with one another, the greater the initial thermodynamic driving force for the corrosion of the more anodic metal.

The severity of the problem is determined by:

- Potential difference between the metals in contact;
- Kinetic factors, such as passivation (where a protective oxide layer forms);
- The ratio of the anodic surface area to the cathodic surface area.

So follow 2 general rules for corrosion protection:

- Avoid unnecessary use of dissimilar metals in electrical contact;
- Keep the anode to cathode area ratio as large as possible.

Consider the protection of steel using zinc and chromium coatings. As long as the coating is continuous and defect-free, either metal protects. The difference is if a scratch in the coating occurs. The galvanic series shows that Zn is anodic to steel and should continue to protect the steel. In contrast, Cr is cathodic to steel and so the steel begins to corrode preferentially. The problem is amplified by the small exposed area of the steel, which gives an unfavourable anode-to-cathode area ratio. Car bumpers are Cr plated; hence when rust first appears its volume increases rapidly. Zn-plated steel is a better choice if corrosion resistance is of prime concern. Steel trash cans are galvanised.

Galvanic couples may develop at the microscopic level, e.g. welded stainless steel. Whilst the passive chromium oxide layer is protective, unfortunately during welding some Cr can combine with carbon to produce Cr carbides at grain boundaries. The corresponding decrease in Cr content of the steel adjacent to the grain boundary renders the steel not stainless and anodic with respect to the bulk of the structure. The low anode-to-cathode area ratio is again unfavourable.

A possible remedy is to use a stainless steel with very low C content, or add Ti or Nb to the alloy to "mop" up the C. Also, a post-weld heat treatment can dissolve the Cr carbides and diffuse the Cr back into solution.

Here are several general rules that minimise this form of corrosion:

- Select single-phase alloys;
  - Solid solution strengthen rather work harden an alloy. (Work hardening increases the energy of level of atoms at defects rendering the local region anodic);
  - Avoid small grain sizes if possible;
  - Ensure a homogeneous distribution of the alloying elements;
  - Eliminate any residual stresses;
  - Produce a fully recrystallised large grain structure;
- Use plastic washers to separate dissimilar metals, between steel and copper.

Local anodic regions can form because of oxygen concentration gradients in the electrolyte. A region of higher oxygen content becomes cathodic with respect to the surrounding material. A single drop of water on a metal surface results in the formation of an oxygen concentration cell. On steel, rust can form just outside the waterline.

Pitting and crevice corrosion are localised forms of attack involving oxygen concentration gradients. Presence of chlorine ions increases the severity of the problem. Pits often form under debris, and places of stagnant pools of electrolyte on horizontal sections. Crevice corrosion can occur between metal sheets joined using bolts, screws, or rivets. These forms of corrosion which are difficult to detect, are best overcome by design considerations. Welded joints are preferred in aggressive environments. Avoid sharp corners, etc that favour the formation of stagnant pools. Design to permit free drainage and avoid sediment buildup.

Other methods that can be used to prevent galvanic attack include:

Cathodic protection where the current flow is reversed, i.e. reverse the anode and cathode. The metal to be protected is connected to the negative terminal of a DC power supply. This can be applied to buried steel pipes. A piece of scrap iron is connected to the other side of the voltage source and becomes the anode. Another version involves the use of a sacrificial anode. A galvanic cell is formed by attaching a more anodic metal in electrical contact with the metal to be protected. The anodic metal is sacrificed, e.g. large Zn or Mg plates attached to ocean vessels below the waterline; also, Zn slugs in car radiators.

Protective coatings based on cathodic (galvanic) protection or coatings to physically separate 2 metals in contact. They include grease, oil, waxes; also, porcelain enamels, tar, PTFE, paints, lacquers. Passive oxides, eg., those formed in the anodisation of Al also protect.



If 1 mol of zinc dissolves, the number of electrons released is:  $6.022 \times 10^{23} \times 2$ .

The charge released is  $6.022 \times 10^{23} \times 2 \times 1.602 \times 10^{-19} \text{ C}$  which

$$= 6.022 \times 2 \times 1.602 \times 10^4 \text{ C}$$

$$= 1.93 \times 10^5 \text{ C.}$$

The number of coulombs liberated by the anode is:

$$(136 \text{ kg}) / (0.0654 \text{ kg}) \times 1.93 \times 10^5 \text{ C}$$

$$= (1.36 / 0.0654) \times 1.93 \times 10^8 \text{ C}$$

$$= 4.01 \times 10^8 \text{ C.}$$

If the current is 1A, 1C passes per second. Therefore, the time is:

$$= (4.01 \times 10^8) / (2 \times 60 \times 60 \times 24 \times 365) \text{ years}$$

$$= 6.36 \text{ years.}$$

10. (a) Survival probability of the larger component  $V$  (the compressor blade) is given by:

$$P_S(V) = \exp \{-(V/V_0) (\sigma/\sigma_0)^m\}$$

Taking natural logs

$$\ln P_S(V) = -(V/V_0)(\sigma/\sigma_0)^m$$

Equate *survival probabilities* of the 2 samples of *different size* and re-arrange the design equation to show:

$$(\sigma_{comp} / \sigma_{test}) = (V_{test} / V_{comp})^{1/m}$$

where  $\sigma_{testpiece}$  is 250MPa and  $V_{testpiece}$  is 0.1 the volume of the blade.

For the same probability of survival (95%) and 10 fold increase in volume, the strength of the blade is reduced from about **250 to 200 MPa**.

(b-c) Make smaller grained parts to increase the tensile strength. The grain boundary acts as a barrier to the growth of cracks. Reduce the porosity content of the ceramic during manufacture by careful control of temperature and pressure in sintering components. Introduce ductile particles or fibres. Avoid notches and holes. Improve surface finish; load in compression (if at all possible); avoid point loading; allow for thermal expansion mismatch in a ceramic-metal assembly; avoid large thermal stresses and temperature gradients; characterise defects; and proof test articles to increase survival probability by weeding out the weak ones. Consideration must also be given to the form (or shape and size), and stress-state of the ceramic component. Basic energy absorbing mechanisms to *increase* the toughness of the ceramic (or *decrease* stress intensity  $K$  at crack tip) include: presence of fibres or whiskers to bring about crack deflection (and blunting) in front of the crack tip; crack bridging processes behind (in the wake) of the crack tip with fibres ductile or otherwise; stress-induced transformation toughening around the crack tip.

11. (a)  $\sigma = pR/t = (1.5 \times 0.84)/0.014 = 90\text{MPa}$

$$\sigma = 90\text{MPa}$$

(b)  $\sigma_f = K_{Ic}/(\pi a)^{1/2} = 45/(\pi 0.01)^{1/2} = 257 \text{ MPa}$

$$p = \sigma t/R = (257 \times 0.014)/0.84 = 4.3\text{MPa}$$

**This is nearly 3 times greater than the allowable design pressure.**

(c) Conclusion: the relief safety valve must have become inoperative and the vessel was over-pressurized.

(d) Leak before break means that the critical crack depth for fast fracture (catastrophic failure) of a pressure vessel is greater than its wall thickness. That is to say, the crack will penetrate the wall thereby causing escape of the air or gas under controlled decreasing pressure. In a fatigue situation, where a crack can grow over time, safety can be ensured by arranging that a crack is just long enough to penetrate the wall of the vessel and remain stable. Leakage can therefore be observed.

(e) This condition is achieved by setting  $a = t$ :

$$\sigma = \frac{K_{IC}}{\sqrt{\pi t}}$$

Furthermore, the wall thickness  $t$  of the vessel must be sufficiently thick that pressure  $p$  is contained without the vessel yielding:

$$t \geq \frac{pR}{2\sigma_y}$$

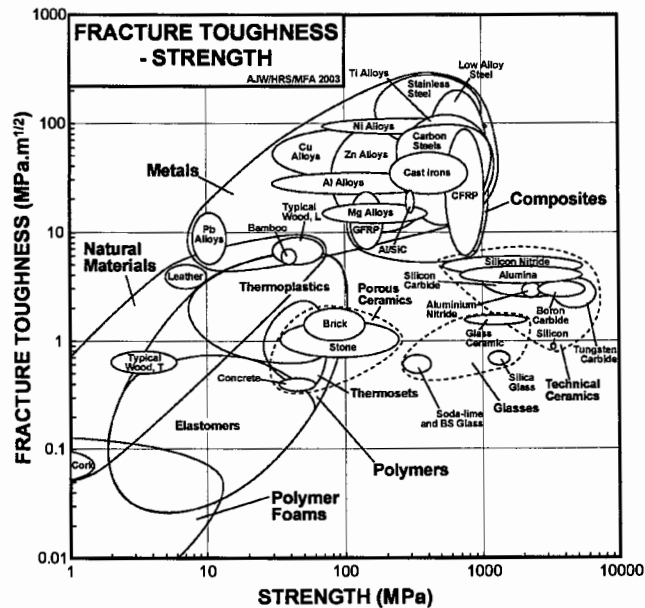
Substituting this equation into the one above:

$$p \leq \frac{1}{\pi R} \left( \frac{K_{IC}^2}{\sigma_y} \right)$$

(f) The pressure carried most safely is when the material selected has the greatest value of:

$$M_I = \frac{K_{IC}^2}{\sigma_y}$$

(g)



The preliminary choice includes all materials above the diagonal line of slope =  $\frac{1}{2}$ . And above the limiting yield stress of 200 MPa. This targets the choice to stainless steel and low alloy steels.

12. (a) The 3 dominant mechanisms are: work hardening, solid solution strengthening, and precipitation strengthening. All of them work by providing “pinning points” - obstacles which hinder dislocation motion. Work hardening increases dislocation density, thereby creating entanglements of dislocations where they intersect. Solid solution strengthening uses individual atoms distributed in the lattice to impede dislocation motion. Both substitutional and interstitial solute atoms perturb the atomic bonds in the lattice around them. Slip between planes becomes difficult. Precipitation hardening involves embedding obstacles of fine particles or compounds in the lattice. Dislocations encountering them on many slip planes are held up and under increasing stress they bow out between precipitates. An applied shear stress forces the dislocation between these 2 obstacles. Once a large enough stress is attained corresponding to a large enough bulge, the dislocation can easily expand further. The dislocation escapes and yielding occurs. Decreasing the spacing between 2 neighbouring precipitates results in a higher shear stress to bring about this phenomenon of dislocation bowing. If dislocation loops are left round each of the 2 precipitates, the effective spacing has decreased and an additional applied stress is necessary to get the second and subsequent dislocations to bulge through the gap.

(b) Cold rolled Al-Mn-Mg alloy are work hardened by the rolling process, and Mn and Mg give solid solution hardening. A 60-40 Cu-Ni alloy uses strong solid solution hardening. Quenching and tempering a medium carbon steel forms finely dispersed precipitates of iron carbide giving effective precipitation strengthening. Alloy steels exploit solid solution strengthening and additional carbide precipitates.

(c) Other examples include:

Work hardening: stainless steels. Solid solution hardening: Cu-Zn brass and Cu-Sn bronzes, stainless steels, most casting alloys Mg, Zn, Al, Ti. Precipitation hardening: alloy steels, tool steels, high temperature Ni alloys, “heat-treatable” Al alloys.

(d) To find the particle spacing, consider a cube of side length  $L^*$  with a spherical particle of radius  $r$  at each corner. Given the particle volume fraction (0.05), then:

$$\frac{\left(\frac{4\pi r^3}{3}\right)}{L^{*3}} = 0.05 \Rightarrow L^* = 0.175 \mu\text{m}$$

Knowing the radius of the particle (0.04  $\mu\text{m}$ ), the particle separation (surface-to-surface) distance  $L$  can be determined:

$$L = L^* - 2r = 0.095 \mu\text{m}$$

The yield strength  $\sigma_y$  of a polycrystalline material is related to the shear stress  $\tau_y$  required to move a dislocation on a single slip plane by:

$$\sigma_y = 3\tau_y = \frac{3Gb}{L} = \frac{3 \cdot (26 \times 10^9) \cdot (3 \times 10^{-10})}{0.095 \times 10^{-6}} \approx 246 \text{ MPa}$$

where  $G$  is shear modulus (26 GPa) and  $b$  is burgers vector ( $3 \times 10^{-10}$  m).

Thus the total yield strength of the dispersion strengthened alloy will be given by:

$$30 + 246 = 276 \text{ MPa}$$

(e) (i) If there is non-uniformity in precipitate spacing, those neighbour precipitates that are spaced furthest apart would allow segments of a dislocation to pass through more easily. The effect would be that the alloy has a reduced yield strength.

(ii) Over time at elevated temperature particles would grow in size and a corresponding increase in spacing between neighbouring particles. The yield stress would fall.

*Question 12(d) : solution corrected 02/05/11*

Peter W R Beaumont

26<sup>th</sup> June, 2008